Optical properties of a spherical two-dimensional electron gas in a uniform magnetic field

2004 J. Phys.: Condens. Matter 16 8233

(http://iopscience.iop.org/0953-8984/16/46/010)

INSTITUTE OF PHYSICS PUBLISHING JOURNAL OF PHYSICS: CONDENSED MATTER

J. Phys.: Condens. Matter **16** (2004) 8233–8241 PII: S0953-8984(04)84942-7

Optical properties of a spherical two-dimensional electron gas in a uniform magnetic field

A Goker and P Nordlander

Department of Physics and Department of Electrical and Computer Engineering, Rice Quantum Institute, MS 61, Rice University, Houston, TX 77251-1892, USA

E-mail: nordland@rice.edu

Received 12 August 2004, in final form 6 October 2004
Published 5 November 2004
Online at stacks.iop.org/JPhysCM/16/8233
doi:10.1088/0953-8984/16/46/010

Abstract

Using the random phase approximation, we calculate the plasmon frequencies of an electron gas on a two-dimensional spherical surface in the presence of a weak magnetic field. We show that the magnetic field results in a coupling between electronic states with different angular momentum numbers. This coupling results in a blue-shift of the dipolar plasmon resonance with increasing magnetic field. We also investigate how the plasmon energies vary as a function of the number of electrons and radius of the sphere.

1. Introduction

Metallic shell structures are of considerable theoretical and experimental interest because of their unusual electronic and optical properties [1–5]. In recent years, it has been possible to manufacture spherical shaped nanostructures ranging from fullerene size to nanosized objects such as SiO_2 balls in opals [6], nanoshells [7] and multielectron bubbles [8, 9]. The motion of charged particles on such spheres with constant magnetic field along a given axis of the sphere has been studied previously [10–14]. The energy spectrum has been calculated and the thermodynamical properties, such as magnetization and magnetic susceptibility, have been studied rigorously.

For multielectron bubbles in the absence of an applied magnetic field, the electrons move freely in the direction tangential to the spherical helium surface. The electrons therefore effectively form a spherical two-dimensional electron gas (S2DEG). A S2DEG can also be realized in charge droplets [15] and in doped semiconductor particles if carriers accumulate in a surface layer [16]. In previous work, the many-body properties of such a system have been investigated using the random phase approximation, and the multipole excitation modes of the S2DEG have been calculated [17] and the angular momentum dependent dielectric function of the S2DEG has been derived [18].

Motivated by these recent works, we will analyse the optical response of the S2DEG in the presence of a weak uniform magnetic field. In this regime, we can treat the electronic structure of the system using perturbation theory and obtain a closed expression for the optical polarizability. We investigate how the dipolar plasmon energy is affected as the magnetic field or the number of electrons is changed. We show that the energy of the plasmon resonance increases with increasing magnetic field. We provide a simple physical explanation for the observed magnetic field dependence of the plasmon energies.

We hope that this observation may stimulate experiments measuring the magneto-optic effects of the S2DEG. Although the theoretical approach in the present paper is strictly limited to thin electronic shells, we believe that the physical mechanism responsible for the magnetic field dependence of the plasmon energies will apply also in other electronic shell structures such as metallic nanoshells. If this is the case, the application of magnetic fields will provide an interesting additional means of extrinsic tunability of their plasmonic properties which may enable new nanophotonic applications.

2. Theory

In this section, we will first describe the effect of a weak magnetic field on the ground state of the electron gas [14]. We will then use this result to obtain the response properties of the S2DEG using linear response theory.

The system under investigation is electrons constrained to the surface of a sphere of radius r_0 in the Landau gauge. Throughout this paper, we will assume a closed shell configuration for the ground state of the electron gas, i.e. all the angular momentum states, until the Fermi level is fully occupied with two projections of spin. The Fermi angular momentum number L_F determines the number of electrons in the system via $N = 2(L_F + 1)^2$ and the surface charge density is $\nu = N/4\pi r_0^2$. In the Schrödinger equation, we will use a confining potential of the form $V(r) = 0$ for $r_0 < r < r_0 + \delta r$ and $V(r) \to \infty$ otherwise. If we assume $\delta r \ll r_0$, this potential describes a shell with infinitesimal thickness; thus the radial and angular variables of the Schrödinger equation can be separated. If the Fermi level lies below the first excited level of the radial component of the wavefunction, we can ignore the radial component and put $r = r_0$ in the remaining angular part of the Hamiltonian H_Ω. This requires $\delta r \leqslant \nu^{-1/2}$ and, if satisfied, means that we are dealing with an effectively two-dimensional system. Now, we apply a uniform magnetic field along the z axis of the sphere ($\theta = 0$). Since the system has rotational symmetry, an eigenfunction can be written as $\Psi(\theta, \phi) = \Theta(\theta)\exp(\mathrm{i}m\phi)$, where $m\hbar$ is the eigenvalue of $\hat{L}_z$. We will adopt atomic units in the following analysis ($\hbar = e = m_e = 1$, $c = 137$). The angular part of the Hamiltonian becomes

$$H_\Omega = \frac{1}{2r_0^2}\left[-\Delta_\Omega + 2\mathrm{i}p\frac{\partial}{\partial\phi} + p^2\sin^2\theta\right]. \tag{1}$$

The Schrödinger equation then takes the form

$$\frac{\partial}{\partial\zeta}(1-\zeta^2)\frac{\partial\Theta}{\partial\zeta} + \left[\varepsilon - 2mp - \frac{m^2}{1-\zeta^2} - p^2(1-\zeta^2)\right]\Theta = 0 \tag{2}$$

upon introducing $\zeta = \cos\theta$, the dimensionless energy $\varepsilon = 2r_0^2E$ and the number of flux quanta p encircled by the sphere, which is given by

$$p = \frac{\pi B r_0^2}{\Phi_0}, \tag{3}$$

where $\Phi_0 = 2\pi/e = 2 \times 10^{-15}$ T m^2 is the flux quantum.

The above equation is the well-known spheroidal differential equation [19, 20]. In the absence of magnetic field, this equation reduces to the standard free rotator problem in quantum mechanics and the wavefunctions are the spherical harmonics. In the presence of a weak magnetic field, however, one is able to develop a perturbation theory around the initial wavefunctions as long as $p^2 \leqslant 4l$ to get a series of Zeeman-split $2(2l+1)$ states with energy eigenvalues [14]

$$\varepsilon_{lm\sigma}(p) = l(l+1) + 2pm + \frac{p^2}{2}\left[1 + \frac{m^2}{l^2}\right] + \frac{p^2}{l} + \frac{2\Phi_0}{137\pi} p\sigma + \mathrm{O}(p^4) \tag{4}$$

and normalized wavefunctions

$$\Psi_{lm}(p, \Omega) = \frac{Y_{lm}(\Omega) + \frac{p^2}{l} Y_{l+2,m}(\Omega) + \frac{p^2}{l} Y_{l-2,m}(\Omega)}{\sqrt{1 + \frac{2p^4}{l^2}}} + \mathrm{O}(p^4), \tag{5}$$

where Ω denotes the spherical angles $\Omega = \{\theta, \phi\}$ and (l, m) represents the angular momentum state. In equation (4), the last term represents the contribution from the spin degrees of freedom and σ denotes the projection of the spin. This term is much smaller than the others, and will be neglected in the following.

Our aim in this paper is to use the above perturbed energy eigenvalues and wavefunctions to calculate the dielectric response function using the random phase approximation (RPA). We will investigate the behaviour of the optically active dipolar plasmon energy in the presence of the magnetic field.

In linear response theory, an induced electron density $\rho_{\mathrm{ind}}(p, \Omega, \omega)$ is generated when an external field $V_{\mathrm{ext}}(\Omega, \omega)$ which couples to the electron density is applied. Its spherical components can be written as

$$\rho_{\mathrm{ind}}(p, l, m, \omega) = V_{\mathrm{ext}}(l, m, \omega) D_{\mathrm{R}}(p, l, m, \omega), \tag{6}$$

where $D_{\mathrm{R}}(p, l, m, \omega)$ is the retarded density–density Green function. The Lindhard or independent electron response function $D^0_{\mathrm{R}}(p, l, m, \omega)$ takes the form

$$\begin{aligned} D^0_{\mathrm{R}}(r_0, p, l, m, \omega) = {} & \sum_{l',m'} \sum_{L,M} n(l', m')(1 - n(L, M)) \\ & \times \left| \int Y_{l,m}(\Omega) \Psi^*_{L,M}(p, \Omega) \Psi_{l',m'}(p, \Omega)\, \mathrm{d}\Omega \right|^2 \\ & \times \left(\frac{1}{\omega + \frac{\varepsilon_{l',m'}(p) - \varepsilon_{L,M}(p)}{2r_0^2} + \mathrm{i}\eta} - \frac{1}{\omega + \frac{\varepsilon_{L,M}(p) - \varepsilon_{l',m'}(p)}{2r_0^2} + \mathrm{i}\eta} \right). \end{aligned} \tag{7}$$

In this expression, $n(l', m')$ and $n(L, M)$ denote the occupancy of the initial and final angular momentum states respectively and (l, m) represents the excitation. The quantity η is an infinitesimal damping term and $\varepsilon_{l,m}(p)$ is given by equation (4).

Using the expression (5) for the wavefunctions, the angular integrals can be expressed in Clebsch–Gordon coefficients and Wigner $3j$ symbols. For the present large systems ($L_{\mathrm{F}} > 20$) and small magnetic fields ($p < 5$), the dependence of the energy denominators on m' and M is small and can be neglected. The summations over m' and M in equation (7) can then be

done analytically and the response function takes the form

$$
\begin{aligned}
D^0_{\mathrm{R}}(r_0,\, p, l, \omega) = \sum_{l'} \sum_{L} n(l')(1 - n(L)) \frac{1}{4\pi} \frac{1}{1 + \frac{2p^4}{l'^2}} \frac{1}{1 + \frac{2p^4}{L^2}} \\
\times \Bigg[(2l' + 1)(2L + 1) \begin{pmatrix} l & l' & L \\ 0 & 0 & 0 \end{pmatrix}^2 \\
+ (2l' + 1)(2L + 5) \begin{pmatrix} l & l' & L + 2 \\ 0 & 0 & 0 \end{pmatrix}^2 \frac{p^4}{L^2} \\
+ (2l' - 3)(2L + 1) \begin{pmatrix} l & l' - 2 & L \\ 0 & 0 & 0 \end{pmatrix}^2 \frac{p^4}{l'^2} \\
+ (2l' + 5)(2L + 1) \begin{pmatrix} l & l' + 2 & L \\ 0 & 0 & 0 \end{pmatrix}^2 \frac{p^4}{l'^2} \\
+ (2l' + 1)(2L - 3) \begin{pmatrix} l & l' & L - 2 \\ 0 & 0 & 0 \end{pmatrix}^2 \frac{p^4}{L^2} \Bigg] \\
\times \left(\frac{1}{\omega - \frac{\Delta\varepsilon_{L,l'}(p)}{2r_0^2} + \mathrm{i}\eta} - \frac{1}{\omega + \frac{\Delta\varepsilon_{L,l'}(p)}{2r_0^2} + \mathrm{i}\eta} \right)
\end{aligned}
\tag{8}
$$

where the energy denominators are evaluated for $m' = l'$ and $M = l' + 1$,

$$
\Delta\varepsilon_{L,l'}(p) = L(L + 1) - l'(l' + 1) + 2p + \frac{p^2}{2} \left(\frac{(l' + 1)^2}{L^2} - 1 \right) + p^2 \left(\frac{1}{L} - \frac{1}{l'} \right). \tag{9}
$$

The calculation of the RPA dielectric function can be accomplished in a straightforward manner by using a Dyson series once we know the Lindhard response function given by equation (8). The RPA dielectric function has the form

$$
\epsilon_{\mathrm{RPA}}(r_0,\, p, l, \omega) = 1 - v(l, r_0) D^0_{\mathrm{R}}(r_0,\, p, l, \omega). \tag{10}
$$

3. Results and discussion

In the many-body theory of the two-dimensional homogeneous spherical electron gas, two types of excitation are possible: single-particle excitations and plasmons. In the first case, the imparted angular momentum is absorbed completely by a single electron and it gets excited to a higher angular momentum state. On the other hand, a plasmon is a collective excitation involving all the conduction electrons. In both single-particle excitations and the plasmons, the excitation is characterized by the angular momentum l and energy ω.

Plasmon resonances appear when the dielectric function defined by equation (10) satisfies the following two equations:

$$
\mathrm{Im}[\epsilon_{\mathrm{RPA}}(r_0,\, p, l, \omega)] = 0, \tag{11}
$$

$$
\mathrm{Re}[\epsilon_{\mathrm{RPA}}(r_0,\, p, l, \omega)] = 0. \tag{12}
$$

The first equation means that $\omega \neq \Delta\varepsilon_{L,l'}(p)/2r_0^2$, i.e., the plasmon energies lie outside the region of single-particle excitations. In order to find the values of plasmon energies, one has to solve equation (12) for successive values of l. In figure 1, we show the calculated plasmon energies in zero magnetic field, ω_l, as a function of l for three spheres with different radii. All spheres contain 882 electrons and $L_{\mathrm{F}} = 20$. As the radius gets larger, the plasmon energies decrease for each mode due to the $1/2r_0^2$ factor in equation (8).

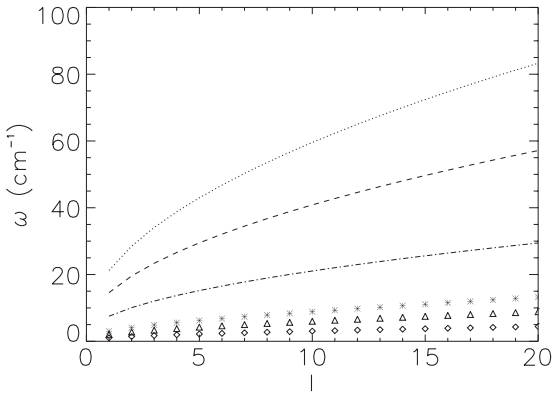

Figure 1. This figure shows the calculated plasmon energies ω_l for the S2DEG as a function of angular momentum l in zero magnetic field. $L_F = 20$ and the number of electrons is 882. The radii of the spheres are 3980 au (stars), 5117 au (triangles) and 7960 au (diamonds). The dotted, dashed and dash–dotted curves represent the plasmon energies obtained from equation (15) by using these parameters respectively.

For S2DEG electrons localized in a Wigner lattice, plasmons of another type can also appear [21]. The system can be viewed as a metallic nanoshell with infinitesimal thickness [22–24]. A general semiclassical approach (SCA) was developed and applied to describe collective resonances in metallic shell structures [25, 26]. For a spherical shell geometry with a step-function charge density, the SCA predicts two collective oscillation modes for each component of the angular momentum. The energies of these plasmons are given by

$$\omega_{l\pm}^2 = \omega_s^2\left[1 \pm \frac{1}{2l+1}\sqrt{1+4l(l+1)x^{2l+1}}\right] \tag{13}$$

where $\omega_s = \sqrt{2\pi e^2 n_0/m_e}$ is the surface plasmon energy and x is the aspect ratio defined as the ratio between the inner and outer radii of the metallic shell. The quantity n_0 represents the volume electron density. We will be considering only ω_{l-} in equation (13) since the other one lies far higher in the energy spectrum and would be very difficult to detect experimentally.

If the electron layer has a thickness d of the order of a few nanometres, just like the case for a multielectron bubble, we can rewrite equation (13) as

$$\omega_{l-}^2(\nu, d, r_0) = \frac{2\pi e^2 \nu}{d m_e}\left[1 - \frac{1}{2l+1}\sqrt{1+4l(l+1)\left(\frac{r_0-d}{r_0}\right)^{2l+1}}\right], \tag{14}$$

and take the limit $d \to 0$ to obtain

$$\omega(l) = \sqrt{\frac{Ne^2}{m_e r_0^3}\frac{l(l+1)}{2l+1}}. \tag{15}$$

This result is in perfect agreement with the plasmon dispersion relation derived by Klimin *et al* using a simple harmonic oscillator model [27]. In figure 1 we also show for comparison the plasmon energies which were obtained by inserting the same parameters as we used to solve equation (12) in (15). The difference in plasmon energies may be a useful way of probing the Wigner lattice and electron liquid phases of electrons on a spherical surface.

Throughout the rest of the paper, we will concentrate on the dipolar plasmon energy in a finite magnetic field since in the long wavelength limit, light excites only this mode. This means that we have to solve equation (12) for $l = 1$. We now determine the range over which

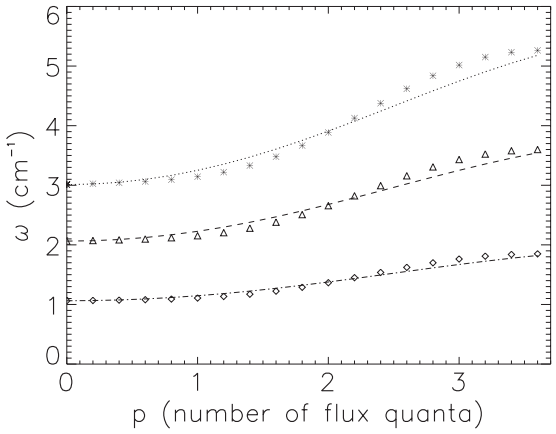

Figure 2. This figure shows the dependence of dipolar plasmon energy on the magnetic field for three different spheres with $L_F = 20$ and 882 electrons. The x axis shows p, the number of flux quanta piercing through the sphere. The radii of the spheres are 3980 au (stars), 5117 au (triangles) and 7960 au (diamonds). The dotted, dashed and dash–dotted curves represent the fits obtained by using equation (16) for these parameters respectively.

we should carry out summations over initial state l' and final state L in the five $3j$ symbols in equation (8). We need to include only those terms for which the Wigner $3j$ symbol is not zero in each case.

We can now start considering each Wigner $3j$ symbol separately. The first term which involves $\left(\begin{smallmatrix} l & l' & L \\ 0 & 0 & 0 \end{smallmatrix}\right)^2$ is the only term that survives in the limit of zero magnetic field where the other four terms with p dependence vanish. This Wigner symbol is zero unless $|L - l'| \leqslant 1 \leqslant L + l'$, which implies that the l' summation for this term runs from $L_F - 1$ to L_F while the L summation runs from l' to $l' + 1$. Obviously, the only allowed one-particle excitations here range from L_F to $L_F + 1$. The next two terms involve $\left(\begin{smallmatrix} l & l' & L+2 \\ 0 & 0 & 0 \end{smallmatrix}\right)^2$ and $\left(\begin{smallmatrix} l & l'-2 & L \\ 0 & 0 & 0 \end{smallmatrix}\right)^2$. They vanish unless $|L+2-l'| \leqslant 1 \leqslant L+l'+2$ and $|L-l'+2| \leqslant 1 \leqslant L+l'-2$ respectively. These inequalities can never be satisfied since the final angular momentum state L is always greater than the initial l'; hence these excitations do not contribute in summations over initial and final angular momentum states.

Finally, let us consider the remaining two terms, namely those that involve $\left(\begin{smallmatrix} l & l'+2 & L \\ 0 & 0 & 0 \end{smallmatrix}\right)^2$ and $\left(\begin{smallmatrix} l & l' & L-2 \\ 0 & 0 & 0 \end{smallmatrix}\right)^2$. They vanish unless $|L-l'-2| \leqslant 1 \leqslant L+l'+2$ and $|L-l'-2| \leqslant 1 \leqslant L+l'-2$ respectively. This means that the summation over l' for these terms runs from $L_F - 3$ to L_F while the summation over L runs from l' to $l'+3$. For example, an excitation from L_F to L_F+3 is allowed for these terms even though we are exciting the sphere with an $l = 1$ mode. This is a consequence of the magnetic field which introduces a coupling between $l = 1$ and 3 modes. In the absence of a magnetic field, $p = 0$ and these two terms vanish, and the $l = 1$ and 3 modes decouple.

In figure 2 we show the dipolar plasmon energy as a function of the number of flux quanta piercing through the sphere for three different radii for an electron density corresponding to $L_F = 20$. The magnetic fields corresponding to $p = 1$ for these systems are 143 G ($r_0 = 3980$ au), 86.5 G ($r_0 = 5117$ au) and 35.75 G ($r_0 = 7960$ au). As the magnetic field is increased, the dipolar plasmon energy starts increasing from its zero-field value which is just the $l = 1$ plasmon to a value somewhere between the zero-field values of ω_1 and ω_3. For example, $\omega_1 = 1.06$ cm^{-1} and $\omega_3 = 1.71$ cm^{-1} for $r = 7960$ au in figure 2. For finite

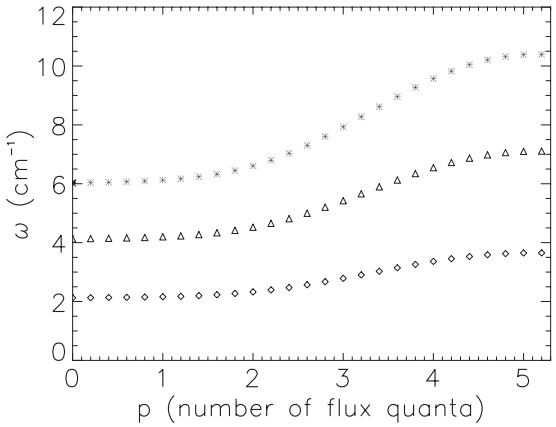

Figure 3. This figure shows the dependence of the dipolar plasmon energy on the magnetic field for three different spheres with $L_F = 41$ and 3528 electrons. The x axis shows p, the number of flux quanta piercing through the sphere. The radii of the spheres are 3980 au (stars), 5117 au (triangles) and 7960 au (diamonds).

magnetic field, the $l = 1$ and 3 modes are coupled and as the strength of the field increases, so does the weight of the $l = 3$ contribution resulting in the increasing blue-shift of the dipolar plasmon mode as a function of the magnetic field. We should also point out that the blue-shift is larger for the same number of flux quanta for smaller spheres. The reason for this is that for fixed p and L_F, the deviation from the plasmon energy at zero magnetic field is controlled by the multiplication factor $1/r_0^2$ in equation (8).

In figure 3, we show the magnetic field dependence of the dipolar plasmon energies for the same size spheres as in figure 2 but with electron densities four times larger, i.e. $L_F = 41$. The zero-field plasmon energies for all radii are about twice as large as in figure 2 due to the linear dependence on the Fermi angular momentum number in the Lindhard response function. In essence, figures 2 and 3 together reveal that the outcome of changing the radius while keeping the number of electrons constant is to rigidly shift the curve up or down.

The last point we have to touch upon as regards these figures is the strength of the magnetic field where the perturbative approach fails. We should recall the perturbed wavefunction equation (5) in order to understand this. Since all excitations take place around L_F, the most strongly contributing angular momenta l are those close to L_F. This means that when p^2 starts approaching L_F, the second and third terms in the perturbed wavefunction become comparable to the first one due to the p^2/l factor. In this limit, our current first-order perturbative treatment fails and higher angular momentum spherical harmonics need to be included. For this reason, we only plotted our figures up to the point where the dipolar plasmon energy saturated. This corresponds to $p = 3.6$ in figure 2 where $L_F = 20$ and $p = 5.2$ in figure 3 where $L_F = 41$. Our present treatment is valid up to these p values. We believe that the saturation in the dipolar plasmon energies is an artefact of first-order perturbation theory and that the plasmon energies would continue to increase with p if we used a higher order perturbation theory.

Next, we will investigate the behaviour of the dipolar plasmon energy as a function of the number of electrons for constant radius and try to elucidate the nature of the mixing between different modes explicitly for a weak magnetic field. In figure 4 we plotted the $l = 1$ and 3 plasmon energies in zero magnetic field for a sphere of radius 3980 au alongside the dipolar plasmon energy when a uniform magnetic field of 0.029 T is applied. The plasmon energies are proportional to the square root of the number of electrons in zero magnetic field. In the

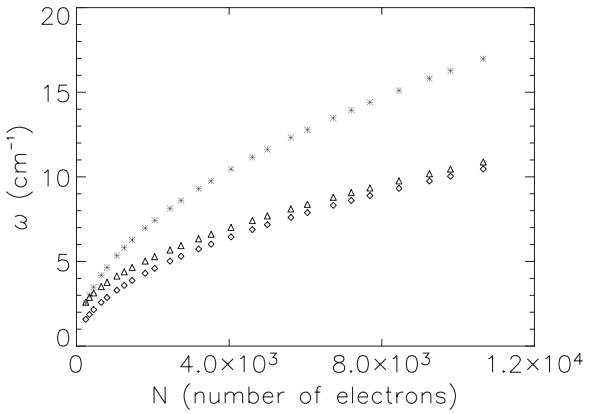

Figure 4. This figure shows the dependence of the dipolar plasmon energy on the number of electrons on the sphere. The radius is constant and 3980 au. Diamonds and stars denote the plasmon energies for $l = 1$ and 3 modes respectively in zero magnetic field. Triangles represent the dipolar plasmon energies when a magnetic field of 0.029 T is applied on the sphere.

presence of a magnetic field, the dipolar plasmon mode consists of an admixture of $l = 1$ and 3 modes. The figure reveals that as the number of electrons increases, the weight of the $l = 3$ mode decreases and the plasmon energy approaches that of the zero-field $l = 1$ plasmon. We can explain this by considering equation (8). The contribution of the $l = 3$ mode is contained only in the last two terms. Increasing the number of electrons on the sphere means increasing the Fermi angular momentum number L_{F}. For example, $N = 4050$ and 10 658 correspond to $L_{\mathrm{F}} = 44$ and 72 respectively in figure 4. Thus for fixed p the factors p^4/L^2 and p^4/l'^2 in the last two terms in equation (8) decrease, which reduces the weight of the $l = 3$ contribution in the plasmon mode.

Finally, we will try to demonstrate the nature of the coupling between ω_1 and ω_3 modes in the presence of a magnetic field by using a simple qualitative equation which has the form

$$\omega_1(p) = \frac{\omega_1 + \frac{p^2}{L_{\mathrm{F}}}\omega_3}{\sqrt{1 + \frac{p^4}{L_{\mathrm{F}}^2}}}. \tag{16}$$

This equation is reminiscent of the perturbed wavefunctions that we used in our RPA calculations and phenomenologically describes the coupling of the $l = 1$ and 3 plasmons for finite magnetic field. In figure 2, we plotted this equation alongside the numerically calculated plasmon energies for three spheres with different radii. $L_{\mathrm{F}} = 20$ and the number of electrons is 882 for all spheres. It is clear from this figure that this phenomenological equation agrees very well with the numerical data that were obtained by solving equation (12).

Although the present application concerned the magnetic field dependence of the optically active dipolar plasmon, we expect higher multipolar plasmons to also exhibit a magnetic field dependence. For a given angular momentum l, the mixing of electronic wavefunctions of different angular momentum, equation (5), will result in a plasmon mode containing also $l-2$ and $l+2$ components. Since ω_l is a non-monotonic function of l, the magnetic field dependent mixing will introduce a magnetic field dependent shift of the plasmon resonances.

4. Conclusions

In this paper, we investigated the optical properties of a two-dimensional electron gas constrained on a spherical surface in the presence of a weak uniform magnetic field which

causes a Zeeman shift in the electronic energy levels. We treated this problem perturbatively within the random phase approximation scheme. We concentrated on the behaviour of the dipolar plasmon energy in particular. We showed that there is a blue-shift in this plasmon mode compared to its value at zero magnetic field and that the shift tends to increase as a function of the magnetic field. This blue-shift can be explained as a magnetic field strength dependent mixing between the ω_1 and ω_3 plasmons. Although the present application concerned thin electronic shell structures, the physical mechanism responsible for the magnetic field dependence of the plasmon energies may apply also for nanoparticles of finite shell thickness such as metallic nanoshells. A magnetic field induced tunability of the dipolar plasmon energy of metallic nanoparticles may be useful in developing nanophotonics applications such as magneto-optical switches. Further generalizations of this model to electronic shells of finite thickness are left for future studies.

Acknowledgments

This work was supported by the Robert A Welch foundation under the grant C-1222, and by the Multi-University Research Initiative of the Army Research Office. It is a pleasure to acknowledge valuable discussions with C Dutta and computational help from C Oubre. We are also very grateful to J Tempere for his valuable comments on the different phases of multielectron bubbles and Wigner crystallization.

References

[1] Haldane F D M 1983 *Phys. Rev. Lett.* **51** 605
[2] Fano G, Ortolani F and Colombo E 1986 *Phys. Rev.* B **34** 2670
[3] Melik-Alaverdian V, Bonesteel N E and Ortiz G 1997 *Phys. Rev. Lett.* **79** 5286
[4] Yiang J and Su W 1997 *J. Mod. Phys.* B **11** 707
[5] Prodan E, Radloff C, Halas N J and Nordlander P 2003 *Science* **302** 419
[6] Vlasov Y A, Astratov V N, Karimov O Z, Kaplyanskii A A, Bogomolov V N and Prokofiev A V 1997 *Phys. Rev.* B **55** R13357
[7] Averitt R D, Sarkar D and Halas N J 1997 *Phys. Rev. Lett.* **78** 4217
[8] Volodin A, Khaikin M and Edel'man V 1977 *JETP Lett.* **26** 543
[9] Albrecht U and Leiderer P 1987 *Europhys. Lett.* **3** 705
[10] Aoki H and Suezawa H 1992 *Phys. Rev.* A **46** R1163
[11] Kim J H, Vagner I D and Sundaram B 1992 *Phys. Rev.* B **46** 9501
[12] Ralko A and Truong T T 2002 *J. Phys. A: Math. Gen.* **35** 9573
[13] Bulaev D V, Geyler V A and Margulis V A 2000 *Phys. Rev.* B **62** 11517
[14] Aristov D N 1999 *Phys. Rev.* B **59** 6368
[15] Rayleigh J W 1882 *Phil. Mag.* **14** 184
[16] Sasaki Y, Nishina Y, Sato M and Okamura K 1989 *Phys. Rev.* B **40** 1762
[17] Inaoka T 1992 *Surf. Sci.* **273** 191
[18] Tempere J, Silvera I F and Devreese J T 2002 *Phys. Rev.* B **65** 195418
[19] Flammer C 1957 *Spheroidal Wave Functions* (Stanford, CA: Stanford University Press)
[20] Komarov I V, Ponomarev L I and Slavyanov S Y 1976 *Spheroidal and Coulomb Spheroidal Functions* (Moscow: Nauka)
[21] Tempere J, Klimin S N, Silvera I F and Devreese J T 2003 *Eur. Phys. J.* B **32** 329
[22] Oldenburg S, Averitt R D, Westcott S and Halas N J 1998 *Chem. Phys. Lett.* **288** 243
[23] Graf C and van Blaaderen A 2002 *Langmuir* **18** 524
[24] Sun Y, Mayers B T and Xia Y 2002 *Nano Lett.* **2** 481
[25] Mukhopadhyay G and Lundqvist S 1975 *Nuovo Cimento* B **27** 1
[26] Prodan E and Nordlander P 2003 *Nano Lett.* **3** 543
[27] Klimin S N, Fomin V M, Tempere J, Silvera I F and Devreese J 2003 *Solid State Commun.* **126** 409